AD A138 280 A TECHNIQUE FOR INCREASING THE OPTICAL STRENGTH OF 1/1
SINGLE-CRYSTAL NACl AN..(U) NAVAL WEAPONS CENTER CHINA
LAKE CA J B FRANCK DEC 83 NWC-TP-6464 SBI-AD-E900 318
UNCLASSIFIED F/G 20/5 NL

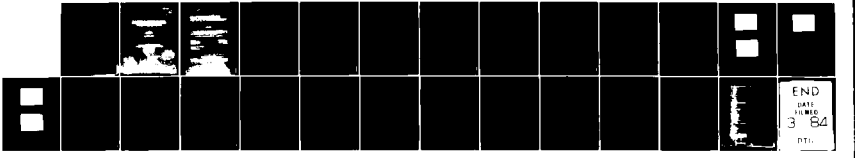

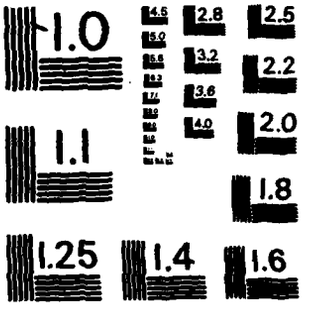

MICROCOPY RESOLUTION TEST CHART
NATIONAL BUREAU OF STANDARDS-1963-A

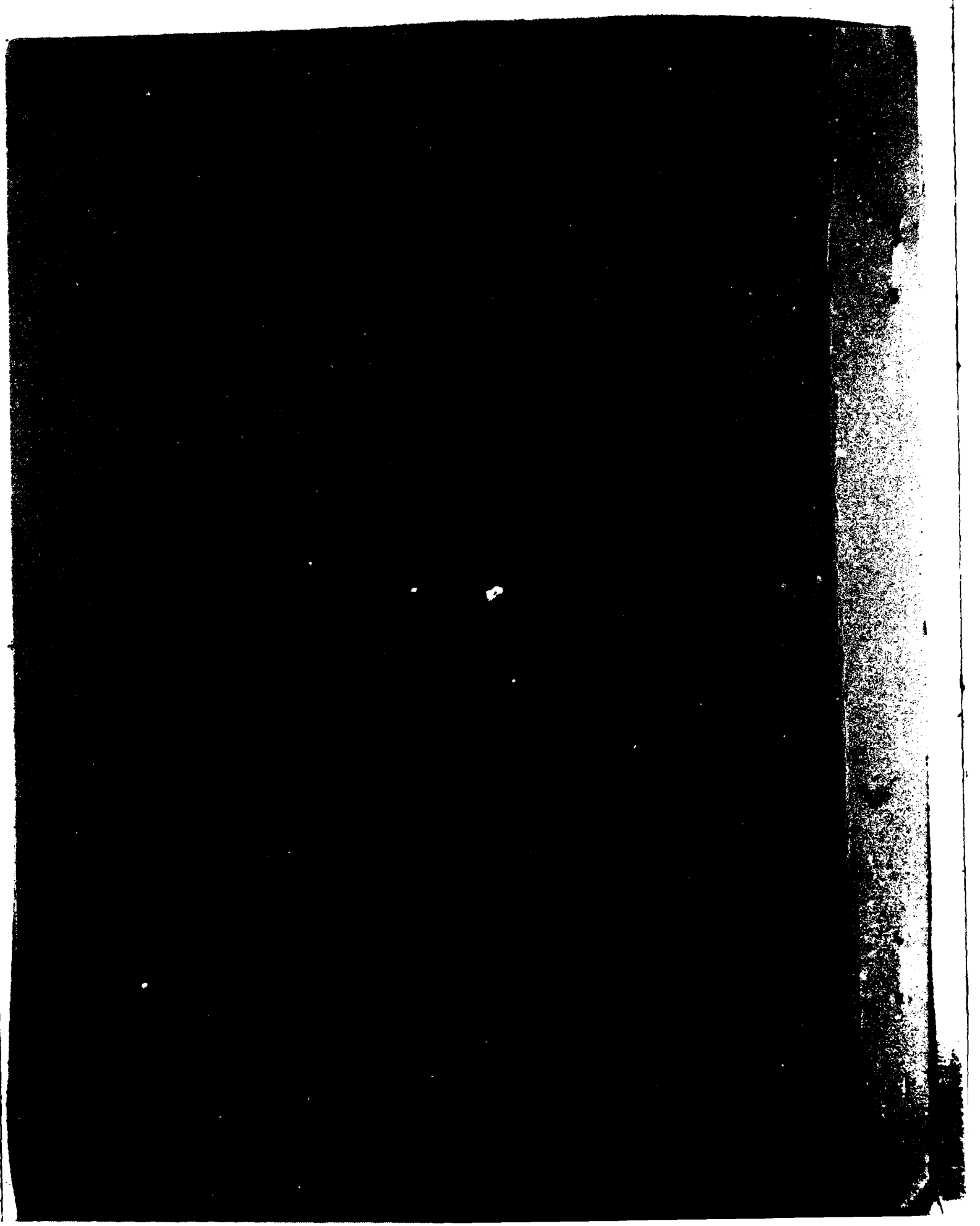

UNCLASSIFIED

SECURITY CLASSIFICATION OF THIS PAGE (When Data Entered)

REPORT DOCUMENTATION PAGE	READ INSTRUCTIONS BEFORE COMPLETING FORM
1. REPORT NUMBER: NWC TP 6464	2. GOVT ACCESSION NO.: AD-A138 280
3. RECIPIENT'S CATALOG NUMBER:	
4. TITLE (and Subtitle): A TECHNIQUE FOR INCREASING THE OPTICAL STRENGTH OF SINGLE-CRYSTAL NaCl AND KCl THROUGH TEMPERATURE CYCLING	5. TYPE OF REPORT & PERIOD COVERED: Interim Report, Fiscal Year 1983
	6. PERFORMING ORG. REPORT NUMBER:
7. AUTHOR(s): J. B. Franck	8. CONTRACT OR GRANT NUMBER(s):
9. PERFORMING ORGANIZATION NAME AND ADDRESS: Naval Weapons Center, China Lake, CA 93555	10. PROGRAM ELEMENT, PROJECT, TASK AREA & WORK UNIT NUMBERS: Program Element 61152N; NWC Program 1601
11. CONTROLLING OFFICE NAME AND ADDRESS: Naval Weapons Center, China Lake, CA 93555	12. REPORT DATE: December 1983
	13. NUMBER OF PAGES: 20
14. MONITORING AGENCY NAME & ADDRESS (if different from Controlling Office):	15. SECURITY CLASS. (of this report): UNCLASSIFIED
	15a. DECLASSIFICATION/DOWNGRADING SCHEDULE:

16. DISTRIBUTION STATEMENT (of this Report)

Approved for public release; distribution unlimited.

17. DISTRIBUTION STATEMENT (of the abstract entered in Block 20, if different from Report)

18. SUPPLEMENTARY NOTES

19. KEY WORDS (Continue on reverse side if necessary and identify by block number)

NaCl	Baking
KCl	Laser damage threshold
Alkali halide	Optical strength
Annealing	Single crystal

20. ABSTRACT (Continue on reverse side if necessary and identify by block number)

See back of form.

DD FORM 1 JAN 73 1473 EDITION OF 1 NOV 65 IS OBSOLETE
S/N 0102-LF-014-6601

UNCLASSIFIED
SECURITY CLASSIFICATION OF THIS PAGE (When Data Entered)

(U) A Technique for Increasing the Optical Strength of Single-Crystal NaCl and KCl Through Temperature Cycling, by Jerome B. Franck. China Lake, Calif., Naval Weapons Center, December 1983. 20 pp. (NWC TP 6464, publication UNCLASSIFIED.)

(U) This report relates a technique for increasing the optical strength of NaCl and KCl single-crystal samples. The 1.06-μm pulsed laser damage thresholds were increased by factors as large as 4.6 for a bulk NaCl single-crystal sample. The bulk laser damage breakdown threshold (LDBT) of the crystal was measured prior to and after heat treatment at 800°C using a Nd:YAG laser operating at 1.06 μm. Bulk and surface LDBTs were also studied on samples annealed at 400°C. These samples showed differences in damage morphology on both cleaved and polished surfaces, and the cleaved surfaces had improved damage thresholds. However, neither the polished surfaces nor the bulk showed improved threshold at the lower annealing temperature.

INTRODUCTION

Optical systems used in the infrared (IR) region of the electromagnetic spectrum often contain optical elements made of NaCl or KCl. Both NaCl and KCl are particularly transparent in the IR region of the spectrum. Where high peak powers of optical energy are used, degradation of optical components can be a problem. This report describes a technique — a baking/cooling process — that was found to increase the optical power densities that NaCl and KCl IR optical elements can withstand.

Recent work has shown that what was previously identified as intrinsic laser-induced breakdown[1,2] is actually caused by material defects.[3-6] It has been shown that special processing during crystal growth can significantly increase the optical strength of the

---

[1] N. Bloembergen. "Laser-Induced Electric Breakdown in Solids," IEEE J. Quantum Electron., Vol. QE-10 (1974), pp. 375-386.

[2] W. L. Smith. "Laser-Induced Damage in Optical Materials," Opt. Eng., Vol. 17 (1978), pp. 489-503.

[3] A. A. Manenkov. "New Results on Avalanche Ionization as a Laser Damage Mechanism in Transport Solids," in Laser Induced Damage in Optical Materials: 1977, ed. by A. J. Glass and A. H. Guenther. National Bureau of Standards Special Publication 509. Washington, DC, Government Printing Office, 1977. Pp. 455-464.

[4] M. J. Soileau. "Frequency and Focal Volume Dependence of Laser-Induced Breakdown in Wide Band Gap Insulators," doctoral dissertation, University of Southern California, Los Angeles, 1979.

[5] M. J. Soileau, M. Bass, and P. H. Klein. "Frequency and Focal Volume Dependence of Laser-Induced Breakdown in Wide Band Gap Insulators," in Laser Induced Damage in Optical Materials: 1979, ed. by H. E. Bennett, A. J. Glass, A. H. Guenther, and B. E. Newnam. National Bureau of Standards Special Publication 568. Washington, DC, Government Printing Office, 1980. Pp. 497-518.

[6] E. W. Van Stryland and others. "Pulse Width and Focal Volume Dependence of Laser-Induced Breakdown," Phys. Rev. B, Vol. 23 (1981), pp. 2144-2151.

crystal.[3,4,7] Manenkov[3] has reported that rapid temperature cycling can substantially increase the laser-induced breakdown thresholds of alkali-halide crystals.

This work reports an independent confirmation of results reported by Manenkov[3] and provides additional details of a treatment used to increase the optical strength of NaCl and KCl. Single-crystal specimens were heated to near-melt temperatures and were rapidly quenched. The laser damage breakdown threshold (LDBT) of these specimens was measured before and after heat treatment, using a pulsed laser (9 ns, full width at half maximum) operating at 1.06 μm. The threshold intensity for laser-induced damage increased by up to a factor of 4.6, depending on the previous history of the samples. This heat treatment improved the bulk optical strength of the specimens but destroyed the optical surfaces.

A study of lower temperature cycling was performed so that its effect on bulk and surface LDBTs could be observed. A change in the surface damage morphology was found after heat treatment for both cleaved and polished surfaces. The LDBT of the cleaved surfaces showed significant improvement after low temperature cycling. However, the LDBT of the polished surfaces and the crystal bulk were essentially unaffected.

BACKGROUND

Previous work[3] investigated electron avalanche as a laser damage mechanism in alkali halides. Manenkov[3] found that suitable thermal treatment of samples having an initially low laser damage threshold could greatly increase the laser damage threshold. This study examined the frequency dependence and temperature dependence of laser damage thresholds of alkali halides. Manenkov's result was found to hold true at all the wavelengths under study (0.69 to 10.6 μm) except at 10.6 μm. Further, samples with a high initial laser damage threshold were unaffected by heat treatment. Only heat-treated samples which were rapidly cooled showed improvement. After repeating the heat treatment process, but allowing a longer cooling period, the samples reverted to their original low laser damage threshold.

---

[7] S. D. Allen and others. "Pulsed CO_2 Laser Damage Studies in RAP Grown KCl," in Laser Induced Damage in Optical Materials: 1974, ed. by A. J. Glass and A. H. Guenther. National Bureau of Standards Special Publication 414. Washington, DC, Government Printing Office, 1974. Pp. 66-76.

A more comprehensive investigation of the heat treatment processes was needed to determine critical features of the annealing process and to better define the physical mechanisms involved. This experiment explored several cooling rates associated with near-melt temperatures.

HEAT TREATMENT

Samples used in the study were of single-crystal "laser grade" and "spectroscopic grade" NaCl and KCl from Harshaw Chemical Company.* The samples were mounted for heat treatment as follows. Samples of two different sizes, 2.0 × 2.0 × 2.0 cm^3 and 2.5 × 2.5 × 5.1 cm^3, were placed in a quartz tube oven with an internal diameter of approximately 3.6 cm. In some cases, this necessitated grinding the corners of the sample to allow insertion into the tube. In such cases, the diagonals were reduced to 3.3 cm. The samples contacted the tube directly. Temperatures were continuously monitored by a thermocouple mounted in a 0.05-cm-wide by 0.5-cm-deep hole drilled into one face of each sample. Specimens were continuously flushed with dry nitrogen gas in order to maintain an inert ambient atmosphere during the heat treatment. A small flow rate of 0.05 ℓ/min was maintained to reduce heat loss.

In general, specimens were slowly heated and rapidly cooled. A typical heating and quenching cycle can be seen in Figure 1. Here the total heating and cooling cycle time was about 3.5 hr. Other cycling rates were investigated. In some cases, total cooling rates as high as 80°C/min were used with positive results. After the 3.5-hr treatment, represented by Figure 1, the LDBT was found to increase by a factor of 4.6. Comparable increases were found in other cases where the cycling time was on the order of 30 min. The cycling rate was limited by the development of thermal stress, which became evident at rates > 30°C/min. In all treated samples, stress zones could be seen by the use of crossed polarizers. No stress was found in untreated samples.

Cooling was accomplished by several methods. In one case, the oven was turned off and the sample was allowed to cool to room temperature in a period of about 2 hr. In other cases, the quartz tube was either partially or completely removed from the oven. In some cases, the sample was quickly removed from the center of the oven and placed in a room-temperature part of the quartz outside the oven. The sample was then placed on a 1-kg block of aluminum at room

* Harshaw Chemical Company, 6801 Cochran Road, Solon, OH 44139.

temperature. This procedure produced a cooling rate of approximately 80°C/min. However, such rapid cooling techniques often produce fracturing of the sample.

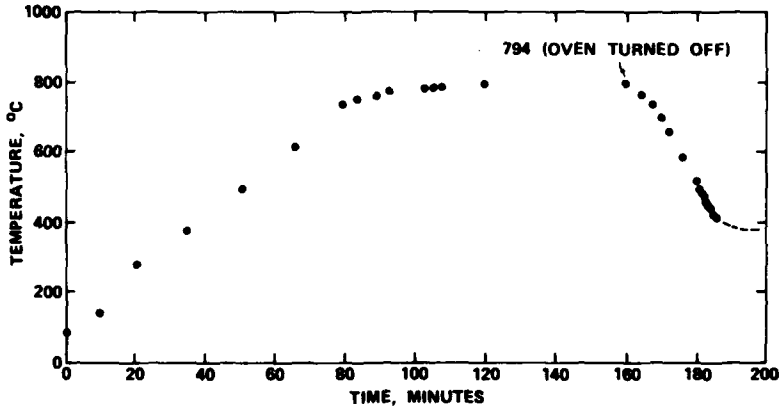

FIGURE 1. Temperature Versus Time of Single-Crystal NaCl. The specimen was heated in a nitrogen atmosphere. It was brought up to 35°C for 10 min, taken to 80°C for 187 min, and heated as shown in the curve above.

Cooling rates from 10°C/min to 80°C/min were investigated. A NaCl sample was cleaved into three pieces, and the LDBT was measured on each. One of the pieces was kept as a control sample, while the other two were put through the temperature cycle as follows. After the two samples were brought to 796°C at a rate of approximately 14°C/min and held there for 10 min, the oven was turned off and one sample was immediately removed from the oven. That sample reached room temperature within 10 min at a rate of approximately 80°C/min; the other sample required 2 hr at a rate of approximately 10°C/min. The samples were repolished and their LDBT remeasured. It was found that the slow-quenched sample had an increase in the LDBT of 1.4, while the quick-quenched sample had a LDBT increase of 4.1.

The above procedure was repeated for intermediate cooling rates of 30°C/min and 40°C/min. The improvement in bulk LDBT increased linearly with cooling rate for rates up to 40°C/min and thereafter remained constant. The results of the cooling rate study for samples brought to near-melt temperature are summarized in Figure 2.

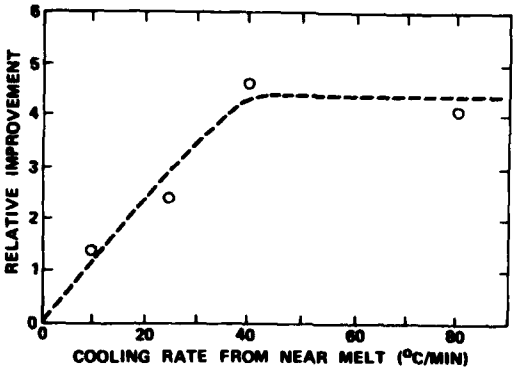

FIGURE 2. Graph of Cooling Rate Versus Relative Improvement in the LDBT for Samples Brought to Near Melt.

Also studied was the effect of cycling NaCl from room temperature to a maximum temperature of 450°C. This temperature was chosen because it has been shown that annealing at 450°C effectively removes color centers.[8] The lower temperature is desirable for several reasons. First, for near-melt temperatures, the surfaces of the samples are sublimed, which substantially degrades the surface optical quality. Second, the extreme temperature variation produces thermal stress, which could be greatly reduced by lowering the cooling rates associated with high maximum temperature.

The LDBT was measured before and after this lower temperature cycling, and LDBT increases of up to 1.3 were measured in the bulk. In this study, heat rates of 7°C/min and cooling rates of approximately 40°C/min were used, and samples were held at 450°C for approximately 20 min. The lack of substantial change in the LDBT suggests that removal of color centers is not associated with the previously referenced annealing process.

The LDBT for front (entrance) surfaces was also compared before and after annealing through the low temperature cycle (450°C maximum). The LDBT of the cleaved surfaces was increased by as much as a factor of four, and the damage morphology was influenced by the heat treatment. The front-surface damage morphology for untreated, cleaved NaCl is seen in Figure 3. Photographs were taken through a

---

[8] T. H. Shulman and W. D. Compton. Color Centers in Solids. New York, Macmillan & Co., 1962.

Nomarski phase contrast microscope. Damage is predominantly in the form of fracturing (from near surface to bulk). Damage on the same sample after treatment is shown in Figure 4; LDBT is four times greater. The damage is primarily a plasma-produced pit, with a circular plasma-etched region about the central pit. All samples were tested in air, and the induced plasma was probably responsible for the degree of plasma etching evidenced.

In Figure 5, the damage morphology for polished, untreated NaCl is seen to be a combination of plasma pitting, plasma etching, and fracturing (at or near the surface). Contrasted in Figure 6 is the same sample after heat treatment, where the damage is typically a plasma-produced pit surrounded by a plasma-etched disk. The same sample can be seen in Figure 7. In this photo (Figure 7), the polarizing prisms are adjusted for maximum contrast to view the plasma-etched disks. In all other photographs, the polarizing prisms are rotated for maximum resolution of surface detail. No change in the LDBT was found in the polished samples. Cooling rates of up to 40°C/min were investigated for surface work, compared with up to 80°C/min used for the bulk.

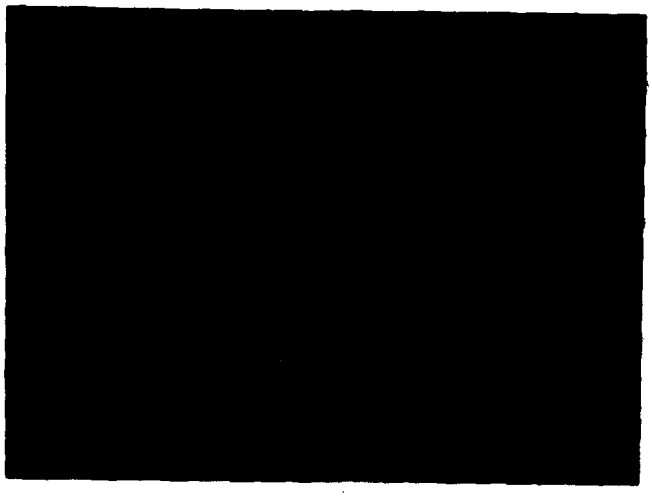

FIGURE 3. Laser Damage at 1.06 μm on an Untreated, Cleaved NaCl Surface. Micrograph taken through Nomarski microscope with prism adjusted for maximum surface detail.

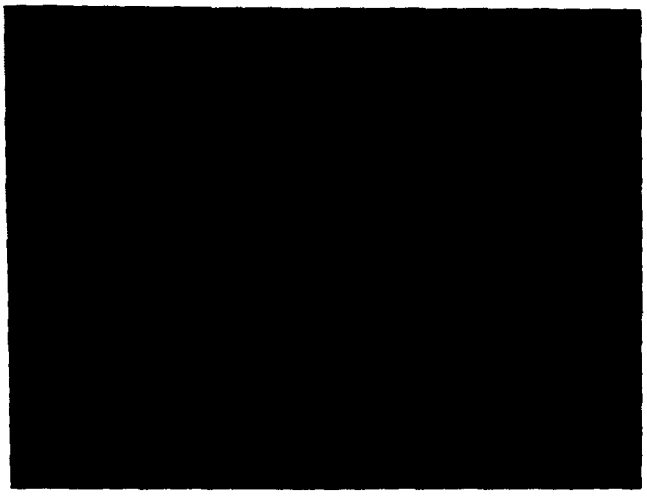

FIGURE 4. Laser Damage at 1.06 μm on Same Surface Shown in Figure 3 After Heat Treatment. Note the marked change in damage morphology.

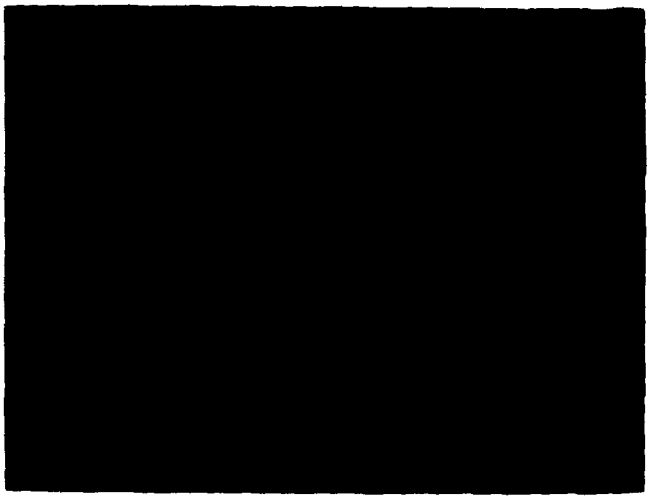

FIGURE 5. Laser Damage at 1.06 µm on a Polished, Untreated NaCl Surface (Sample Number 8, Table III).

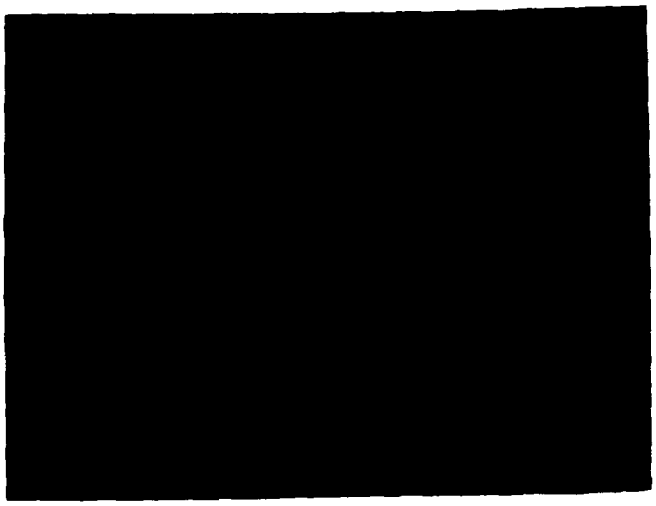

FIGURE 6. Laser Damage at 1.06 μm on Same Surface Shown in Figure 5 After Heat Treatment. Note the marked change in damage morphology.

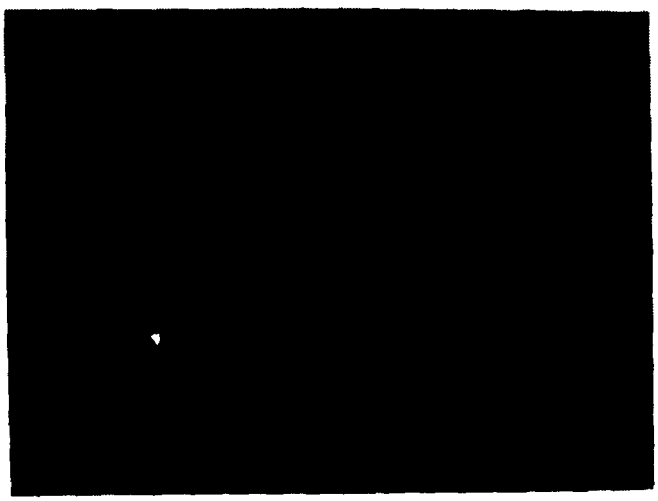

FIGURE 7. Laser Damage at 1.06 μm on Same Surface Shown in Figure 6 with Nomarski Polarizing Prisms Adjusted to Maximum Contrast to Show the Plasma-Etched Region.

Measurements made using newly acquired NaCl and KCl from Harshaw have provided a new insight into the bulk LDBT. These materials were chosen because they have lower metallic-ion contamination. They also have a lower absorption for 10.6-μm radiation, attributed to the lower metallic-ion contamination. Quantitative information on the decreased metallic-ion contamination is unavailable due to proprietary considerations. The new samples were tested, and their bulk LDBT was found to be as high as that of conventional samples that have gone through the heat treatment process. The new samples were put through the treatment process and retested; there was no change in the bulk LDBT.

Manenkov[3] speculates that for samples brought to near-melt temperatures and rapidly quenched, the precipitation of impurity clusters may be retarded. This theory was supported by the study of new samples containing a lower concentration of metallic impurities.

For cleaved samples undergoing low temperature annealing, the improvement in the LDBT may be a result of removal of surface-occluded water in combination with healing of microcracks. No increase in the LDBT was found for polished surfaces. Laser-induced damage in polished surfaces likely is due to absorption by residual polishing material embedded in the surface. The heat treatment described above is probably ineffective in removing such contaminants.

LASER-INDUCED DAMAGE MEASUREMENTS

The bulk laser-induced damage threshold of the specimens was measured before and after heat treatment. The laser used in this work was a Nd:YAG laser operating at 1.06 μm with a pulse width of 9 ns FWHM. The laser was constrained to operate in the TEM_{00} spatial mode by an intracavity aperture. The laser beam was focused onto the specimen by a 162-mm-focal-length BK-7 glass lens used at f/37. The beam radius to the $1/e^2$ point in the intensity profile at the lens focus was calculated to be 26 μm using linear Gaussian optics.

A schematic of the laser damage test station is shown in Figure 8. The station consists of the Nd:YAG laser with its output sent to turning mirror M_1. From M_1 the laser pulse is sent to M_2, which is a dielectric turning mirror used as a beam combiner for a HeNe laser. From M_2 the Nd:YAG and the HeNe laser are made coaxial for alignment and spotting downstream. Approximately 4 percent of the Nd:YAG laser pulse is transmitted through M_2 and is sampled by a Laser Precision detector Model 3232, D_1. This detector is calibrated against a Scientech pyroelectric detector Model 362, D_2. The samples are removed and replaced with the Scientech during calibration.

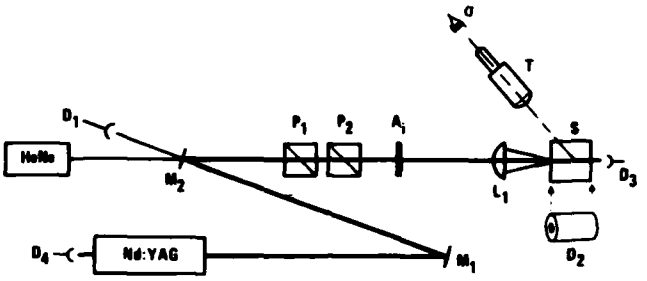

FIGURE 8. Schematic Diagram of the Laser Damage Test Station. Included are the Nd:YAG laser, the coaxial HeNe spotting laser, attenuation section, and sample test site. Detectors D_1 and D_2 measure pulsed energy and calibration, respectively. Fast photodiodes D_3 and D_4 monitor the entrance and exit pulse, respectively, to the sample.

Energy attenuation is accomplished by two means. First, a Glan-Thompson polarizer-analyzer arrangement is used. In Figure 8, P_1 acts as the rotatable polarizer and P_2 acts as the stationary analyzer. P_2 is fixed to maintain a constant polarization output throughout the experiment. Second, thin film fixed attenuators are used at A_1. A 162-mm focal length lens, L_1, was employed. Gross damage and flash were monitored during the experiment by observation through microscope T. Post-experiment observation was performed on a Nomarski phase contrast microscope.

The transmitted pulses were viewed by a fast photodiode, D_3, and compared with a second fast photodiode, D_4. Both photodiodes have rise times of < 1 ns.

The laser damage threshold was taken to be that power level which produced damage at 50 percent of the sites irradiated. This was calculated using an algorithm developed by Porteus.[9] A graphical representation of this method is shown in Figure 9. Each site was

[9] J.O. Porteus, J. L. Jernigan, and W. N. Faith. "Multithreshold Measurement and Analysis of Pulsed Laser Damage on Optical Surfaces," in Laser Induced Damage in Optical Materials: 1977, ed. by A. J. Glass and A. H. Guenther. National Bureau of Standards Special Publication 509. Washington, DC, Government Printing Office, 1977. Pp. 507-515.

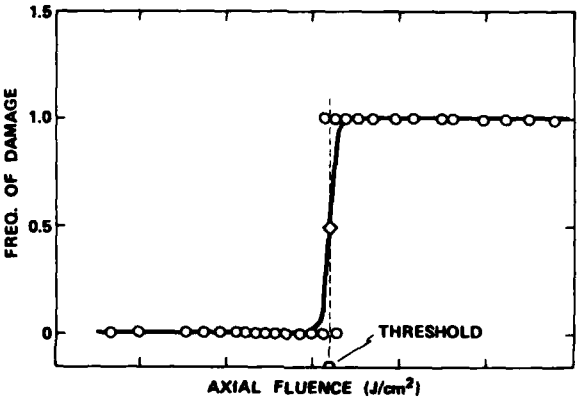

FIGURE 9. Graphic Representation of the Algorithm Used to Calculate the 50 Percent Threshold. A value of 1.0 indicates a a point that damaged at a given fluence; 0 indicates no damage at a given fluence.

irradiated only once, and care was taken to avoid any visible defects in the crystal. It is emphasized that only damage sites that exhibited the type failure that had previously been regarded as intrinsic[1,2] were included in the threshold determination. These were sites that failed at the focal plane of the lens, at the peak of the pulse near threshold, and resulted in abrupt truncation of the pulse transmitted through the specimen.

Truncation of the transmitted pulse was monitored by the fast photodiodes, D_3 and D_4, shown in Figure 8. Similar photographs captured on two Tektronix transient waveform digitizers can be seen in Figures 10 through 13. Figures 10 and 11 show the same pulse before entering and after leaving the sample, respectively. Truncation is evidenced in the output pulse with the input pulse near the damage threshold. Input and transmitted pulses are normalized to the same level. Figures 12 and 13 show the same pulse before entering and after leaving the sample, respectively. Figure 13 shows a more severe truncation than Figure 11 because a visible, absorbing plasma was produced within the sample.

The data from these measurements are summarized in Tables 1 through 3. The power values given are calculated from the measured energy and pulse width. The intensities listed are the peak on-axis intensities calculated using a focal radius of 26 μm; the electric fields are the rms electric fields corresponding to the peak on-axis intensities. The absolute accuracy of the data is estimated to be ±20 percent in the intensity based on uncertainty in the (1) absolute energy measurement, (2) pulse width, and (3) determination of the 50 percent threshold from a data distribution of nonzero width (see Figure 9).

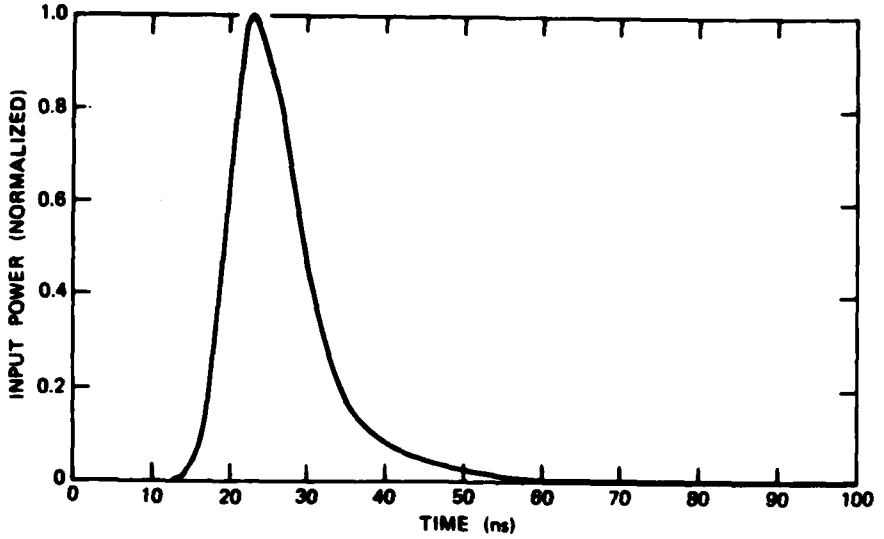

FIGURE 10. Typical Graph of a Normalized Laser Pulse Incident on a Sample. Input power is near the damage threshold.

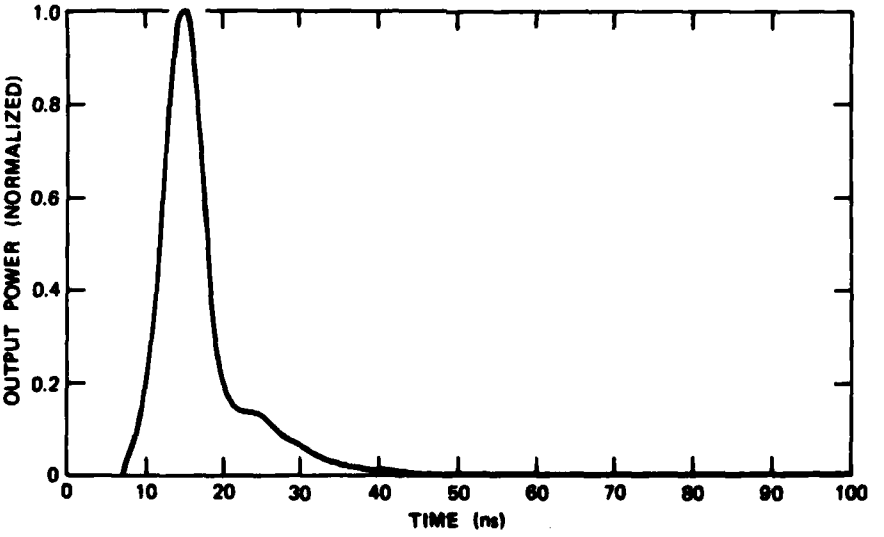

FIGURE 11. The Same Pulse Shown in Figure 10 After Leaving the Sample (Renormalized). Truncation after the initial rise is caused by laser damage.

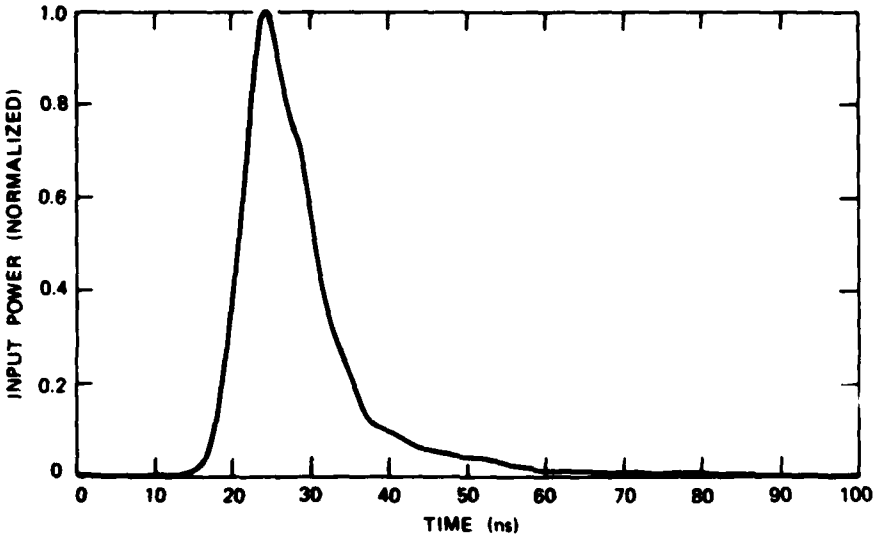

FIGURE 12. Typical Graph of a Normalized Laser Pulse Incident on a Sample. Input power is near the damage threshold.

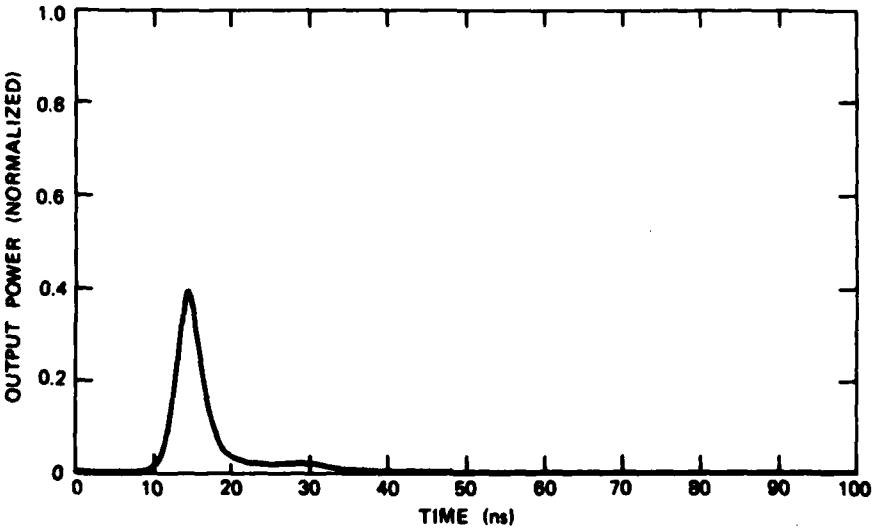

FIGURE 13. The Same Pulse Shown in Figure 12 Exiting the Sample. The output pulse is renormalized to the input pulse. Truncation is severe due to visible plasma.

TABLE 1. Laser-Induced Damage Threshold Before and After Heat Treatment for Bulk Samples at Near-Melt Temperatures.

The relative uncertainties in the thresholds were ±3 percent before treatment and ±5 percent after treatment.

Sample number	Heat treatment	Cooling rate, °C/min	P_B,[a] kW	I_B,[b] 10^9 W/cm^2	E_B,[c] 10^6 V/cm	Relative improvement in LDBT
1	Before	80	74 ± 3	7.0 ± 0.2	1.3 ± 0.02	4.1
	After		305 ± 16	29.0 ± 1.6	2.7 ± 0.07	
2	Before	40	68 ± 2	6.5 ± 0.2	1.3 ± 0.02	4.6
	After		315 ± 16	30.0 ± 0.15	2.7 ± 0.07	
3	Before	40	66 ± 2	6.3 ± 0.2	1.2 ± 0.02	4.4
	After		290 ± 15	27.5 ± 1.4	2.6 ± 0.05	
4	Before	30	70 ± 3	6.7 ± 0.2	1.3 ± 0.02	2.4
	After		168 ± 10	16.0 ± 1.0	2.0 ± 0.04	
5	Before	10	70 ± 3	6.7 ± 0.2	1.3 ± 0.02	1.4
	After		98 ± 5	9.3 ± 0.8	1.5 ± 0.03	

[a] Threshold power defined to be the laser power which produced damage at 50 percent of the irradiated sites.

[b] Peak on-axis intensity calculated using the linear optics focal radius of 26 μm ($1/e^2$ radius of the intensity).

[c] The rms electric field corresponding to I_B using $E_B = 19.41\sqrt{I_B/N}$, where N is the index of refraction.

TABLE 2. Laser-Induced Damage Threshold Before and After Heat Treatment for Cleaved Samples at 450°C Maximum Temperature.

The relative uncertainties in the thresholds were ±3 percent before treatment and ±5 percent after treatment.

Sample number	Heat treatment	P_B,[a] kW	I_B,[b] 10^9 W/cm^2	E_B,[c] 10^6 V/cm	Relative improvement in LDBT
6 Bulk	Before	71 ± 3	6.7 ± 0.2	1.3 ± 0.02	1.3
	After	92 ± 4	8.8 ± 0.7	1.5 ± 0.05	
6 Surface	Before	52 ± 2	5.0 ± 0.1	1.1 ± 0.01	4.0
	After	208 ± 12	20.0 ± 0.9	2.2 ± 0.04	
7 Surface	Before	49 ± 2	4.7 ± 0.1	1.1 ± 0.01	4.2
	After	206 ± 12	19.6 ± 0.9	2.2 ± 0.04	

[a] Threshold power defined to be the laser power which produced damage at 50 percent of the irradiated sites.

[b] Peak on-axis intensity calculated using the linear optics focal radius of 26 μm ($1/e^2$ radius of the intensity).

[c] The rms electric field corresponding to I_B using $E_B = 19.41\sqrt{I_B/N}$, where N is the index of refraction.

TABLE 3. Laser-Induced Damage Threshold Before and After Heat Treatment for Polished Surfaces at 450°C Maximum Temperature.

The relative uncertainties in the thresholds were ±3 percent before treatment and ±5 percent after treatment.

Sample number	Heat treatment	P_B,[a] kW	I_B,[b] 10^9 W/cm^2	E_B,[c] 10^6 V/cm
8	Before	54 ± 3	5.1 ± 0.1	1.1 ± 0.01
8	After	58 ± 3	5.1 ± 0.1	1.1 ± 0.01

[a] Threshold power defined to be the laser power which produced damage at 50 percent of the irradiated sites.

[b] Peak on-axis intensity calculated using the linear optics focal radius of 26 μm ($1/e^2$ radius of the intensity).

[c] The rms electric field corresponding to I_B using $E_B = 19.41\sqrt{I_B}/N$, where N is the index of refraction.

Table 1 shows data on sample numbers 1 through 5 taken to near-melt temperatures. Also shown are the several cooling rates explored and the relative improvement for each sample. Table 2 shows data on cleaved sample numbers 6 and 7 brought to 450°C and cooled at a rate of 40°C/min. The relative improvement in LDBT for the bulk and for the cleaved surface is also shown. In Table 3 data are given for sample number 8. The sample was brought to 450°C and cooled at a rate of 40°C/min. The LDBT for the polished surface exhibited no improvement. In the case of polished samples, a change in the damage morphology was seen (see Figures 4 through 6).

SUMMARY AND DISCUSSION

The laser-induced damage threshold of single-crystal NaCl can be increased by rapidly cooling a crystal heated to near melt (796°C) at a rate of 40°C/min. The reasons for this improvement are not known. Manenkov[3] has speculated that rapid quenching of samples heated to near melting prevents the precipitation of clusters of impurities which may act as initiation sites for electron breakdown. The results reported here for the samples with lower metallic impurity concentration are consistent with Manenkov's explanation. Untreated samples of lower metallic-ion concentrations were found to have a LDBT approximately equal to that of the treated conventional specimens. These samples have shown no change in their LDBT upon heat treatment.

INITIAL DISTRIBUTION

5 Naval Air Systems Command
- ADPO32 (1)
- AIR-00D4 (2)
- AIR-03A (1)
- AIR-310B (1)

2 Chief of Naval Material
- MAT-05 (1)
- NSP-001 (1)

5 Naval Sea Systems Command
- SEA-034D, T. Tasaka (1)
- SEA-99612 (2)
- PMS-405
  - Dr. J. Albertine (1)
  - Dr. D. Finkleman (1)

5 Chief of Naval Research, Arlington
- ONR-200 (1)
- ONR-420, Dr. T. Berlincourt (1)
- ONR-421, Dr. W. J. Condell, Jr. (1)
- ONR-461 (1)
- ONR-471, Dr. A. Diness (1)

1 Commander in Chief, U.S. Pacific Fleet (Code 325)

1 Commander, Third Fleet, Pearl Harbor

1 Commander, Seventh Fleet, San Francisco

2 Naval Ocean Systems Center, San Diego
- Code 9221, L. Eisenman (1)
- Donald Stierwalt (1)

3 Naval Postgraduate School, Monterey
- Code 57FU, Department of Aeronautics, A. E. Fuhs (1)
- Dr. E. Crittenden (1)
- Dr. J. Neighbours (1)

13 Naval Research Laboratory
- Code 5540, Dr. W. S. Watt (1)
- Dr. L. F.Drummeter (1)
- Dr. H. Gandy (1)
- Dr. R. Greene (1)
- Dr. M. Hass (1)
- W. R. Hunter (1)
- Dr. M. Kabler (1)
- Dr. J. C. Kershenstein (1)
- Dr. P. H. Klein (1)
- Dr. R. Patten (1)
- R. Rice (1)
- Dr. A. I. Schindler (1)
- Dr. T. J. Wieting (1)

3 Naval Ship Weapon Systems Engineering Station, Port Hueneme
- Code 5711, Repository (2)
- Code 5712 (1)

1 Naval War College, Newport

1 Office of Naval Research, Boston Branch Office (Dr. F. Quelle)

1 Office of Naval Research, Pasadena Branch Office (Dr. R. Behringer)

4 Army Missile Command, Redstone Arsenal
- DRDMI-HR, Dr. R. L. Hartman (1)
- DRDMI-QRT, Dr. G. J. Hutcheson (1)
- Dr. T. Barr (1)
- Dr. T. Norwood (1)

1 Army Materials and Mechanics Research Center, Watertown (Ceramics Division, Dr. R. N. Katz)
3 Night Vision Laboratory, Fort Belvoir
  Dr. T. Cox (1)
  Dr. G. Hass (1)
  R. Piedmont (1)
1 Office Chief of Research and Development (Air Defense and Missile Division, Dr. R. B. Watson, Chief)
1 Air Force Electronic Warfare Center, San Antonio (ESR)
12 Air Force Weapons Laboratory, Kirtland Air Force Base
  AR, Dr. P. Avizonis (1)
  CA, Dr. A. Guenther (1)
  CL, Capt. A. Luther (1)
  LRE
    Maj. J. Stapp (1)
    Capt. R. House (1)
  Navy High Energy Laser Program Liaison Office
    Dr. J. L. Walsh (1)
    CL (2)
    LR (4)
2 Air Force Wright Aeronautical Laboratories, Wright-Patterson Air Force Base
  AFWAL/MLP (1)
  AFWAL/MLT (1)
3 Under Secretary of Defense Research and Engineering
  I&C, Assistant Director (1)
  Dr. G. Gamota (1)
  J. Persh, Room 3D1085 (1)
3 Defense Advanced Research Projects Agency, Arlington
  Materials Sciences Office, Dr. J. Friebele (1)
  Directed Energy Office
    Col. R. Benedict (1)
    Col. R. Prater (1)
12 Defense Technical Information Center
3 Department of Energy, Oak Ridge
  F. Jones (1)
  R. E. Sladky (1)
  F. Waldrop (1)
5 National Bureau of Standards
  A. Feldman (1)
  R. P. Madden (1)
  K. Mielenz (1)
  C. Teague, Bldg. 220, Rm. A123 (1)
  R. Young (1)
1 National Bureau of Standards, Boulder (R. L. Smith)
2 AVCO Research Laboratory, Everett, MA
  Dr. J. Parks (1)
  Dr. I. Itzkan (1)
2 Battelle Memorial Institute, Pacific Northwest Laboratory, Richland, WA
  Dr. J. S. Hartman, PSL 3000 Area (1)
  R. W. Stewart, Bldg. 231Z (1)
1 CINDAS/Purdue University, West Lafayette, IN
1 Harshaw Chemical Company, Solon, OH
  Dr. O. H. Nestor (1)
  Dr. K. Rosette (1)
1 Harvard University, Cambridge, MA (Division of Engineering and Applied Physics, N. Bloembergen)
2 Honeywell, Inc., Systems & Research Center, Minneapolis, MN
  R. Anderson (1)
  Dr. E. Bernal-G (1)
3 Hughes Aircraft Company, El Segundo, CA (Technical Document Center, B. W. Campbell, Bldg. E1, MS E110)
  Dr. F. McClung (1)
  Dr. J. Rogers (1)
  Dr. S. Scheele (1)

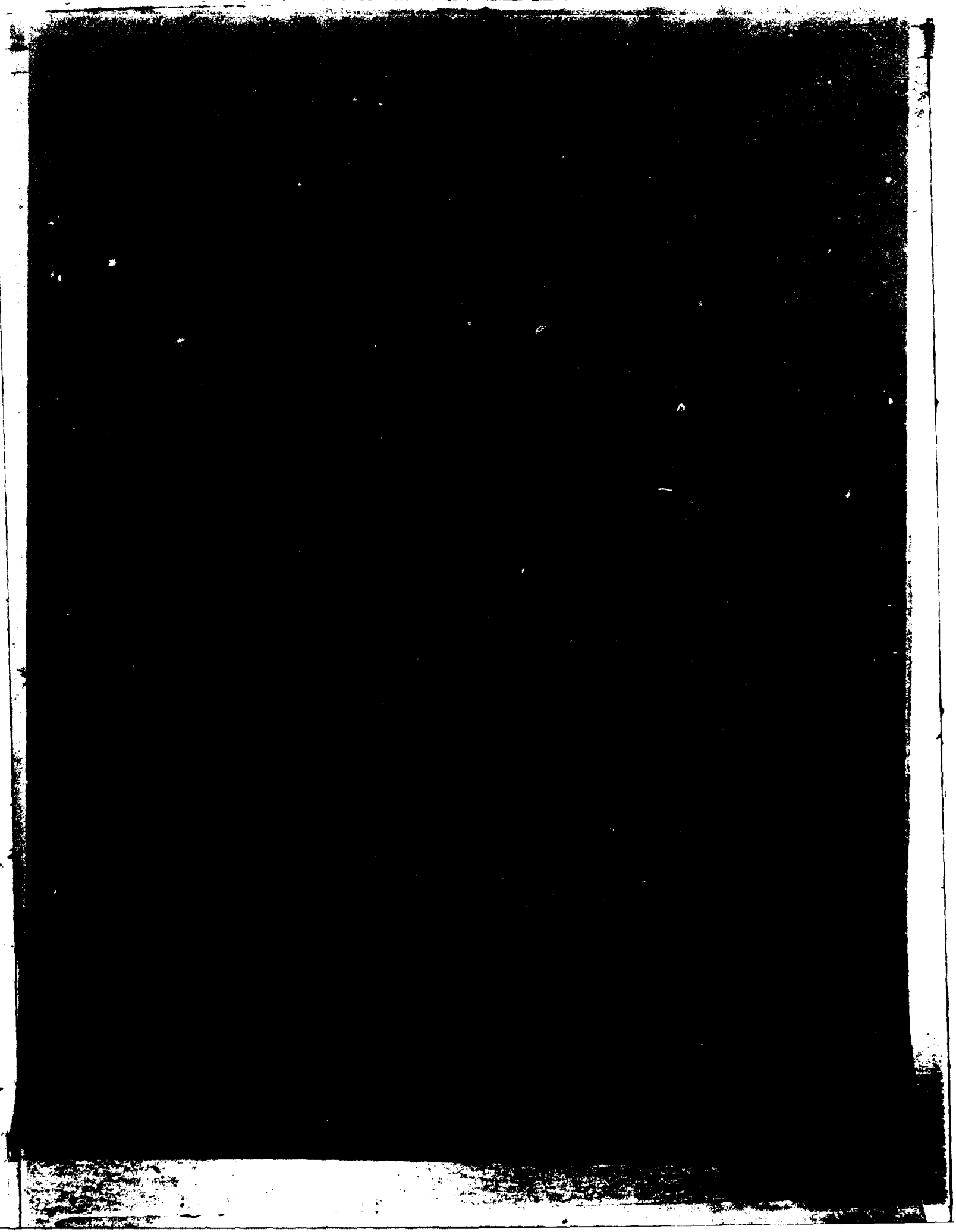

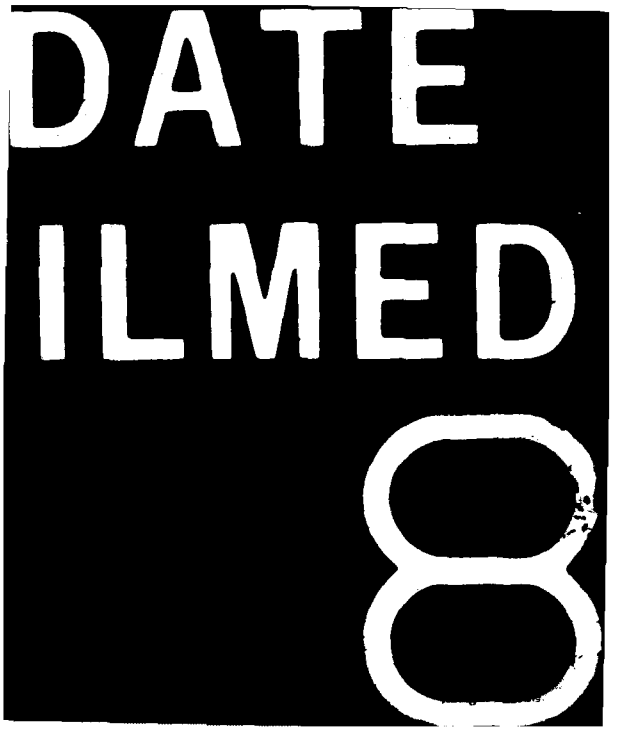
DATE
ILMED
8